

Arabidopsis peroxisomes possess functionally redundant membrane and matrix isoforms of monodehydroascorbate reductase

Cayle S. Lisenbee^{†,‡}, Matthew J. Lingard[‡] and Richard N. Trelease^{*}

School of Life Sciences and Graduate Program in Molecular and Cellular Biology, PO Box 874501, Arizona State University, Tempe, AZ 85287, USA

Received 22 April 2005; revised 23 June 2005; accepted 27 June 2005.

^{*}For correspondence: (fax +1 480 965 6899; e-mail trelease.dick@asu.edu).

[†]Present address: Cancer Center, Mayo Clinic in Scottsdale, Scottsdale, AZ 85259, USA.

[‡]These authors contributed equally to this study.

Summary

The H₂O₂ byproduct of fatty acid catabolism in plant peroxisomes is removed in part by a membrane-associated antioxidant system that involves both an ascorbate peroxidase and a monodehydroascorbate reductase (MDAR). Despite descriptions of 32-kDa MDAR polypeptides in pea and castor peroxisomal membranes and cDNA sequences for several 'cytosolic' MDARs, the genetic and protein factors responsible for peroxisomal MDAR function have yet to be elucidated. Of the six MDAR polypeptides in the Arabidopsis proteome, named AtMDAR1 to AtMDAR6 in this study, 47-kDa AtMDAR1 and 54-kDa AtMDAR4 possess amino acid sequences that resemble matrix (PTS1) and membrane peroxisomal targeting signals, respectively. Epitope-tagged versions of these two MDARs and a pea 47-kDa MDAR (PsMDAR) sorted *in vivo* directly from the cytosol to peroxisomes in Arabidopsis and BY-2 suspension cells, whereas AtMDAR2 and AtMDAR3 accumulated in the cytosol. The PTS1-dependent sorting of AtMDAR1 and PsMDAR to peroxisomes was incomplete (inefficient?), but was improved for PsMDAR after changing its PTS1 sequence from –SKI to the canonical tripeptide –SKL. A C-terminal transmembrane domain and basic cluster of AtMDAR4 were necessary and sufficient for targeting directly to peroxisomes. MDAR activity in isolated Arabidopsis peroxisomes was distributed among both water-soluble matrix and KCl-insoluble membrane subfractions that contained respectively 47- and 54-kDa MDAR polypeptides. Notably, a 32-kDa MDAR was not identified. Combined with membrane association and topological orientation findings, these results indicate that ascorbate recycling in Arabidopsis (and probably other plant) peroxisomes is coordinated through functionally redundant MDARs that reside in the membrane and the matrix of the organelle.

Keywords: Arabidopsis, monodehydroascorbate reductase, peroxisome, peroxisomal targeting signal, reactive oxygen species, tobacco BY-2 cell.

Introduction

One function of plant peroxisomes is the removal of toxic reactive oxygen species, such as H₂O₂, that are produced during the oxidative metabolism that takes place in the matrix of the organelle. A portion of toxic H₂O₂ is removed by a cooperative pair of ascorbate-dependent electron transfer enzymes located at the peroxisomal membrane (Corpas *et al.*, 2001; Donaldson, 2002; del Río *et al.*, 2002). Specifically, ascorbate peroxidase (APX) initiates electron transfer from two molecules of ascorbate to convert H₂O₂ into water. This reaction produces two molecules of

monodehydroascorbate (ascorbate free radical) which can be recycled immediately to reduced ascorbate by monodehydroascorbate reductase (MDAR) via electron transfer from NADH. Alternatively, monodehydroascorbate may disproportionate spontaneously to fully oxidized dehydroascorbate, which is reduced back to ascorbate by the action of a glutathione-dependent dehydroascorbate reductase (Jiménez *et al.*, 1997; del Río *et al.*, 1998). The NADH-dependent dehydrogenase activity of MDAR has been suggested as an important mechanism for the regeneration of

NAD to support the β -oxidation of fatty acids in oilseed glyoxysomes (specialized peroxisomes) (Donaldson, 2002; Mullen and Trelease, 1996).

Compared with its peroxisomal APX counterpart, MDAR is a much less characterized component of the peroxisomal membrane in plants. The association of MDAR catalytic activity with glyoxysomal or peroxisomal membranes has been reported by several groups studying different plant species (Bowditch and Donaldson, 1990; Bunkelmann and Trelease, 1996; Ishikawa *et al.*, 1998; Jiménez *et al.*, 1997; Karyotou and Donaldson, 2005; López-Huertas *et al.*, 1999; Mittova *et al.*, 2000). However, the specific peroxisomal membrane protein(s) (PMPs) responsible for this activity has been identified in only a few cases. For instance, in the membranes of castor glyoxysomes Luster *et al.* (1988) identified an integral 32-kDa polypeptide that exhibited NADH:ferricyanide reductase activity, which was found later to be responsible for the observed NADH-dependent reduction of monodehydroascorbate (Bowditch and Donaldson, 1990). López-Huertas *et al.* (1999) provided more convincing evidence for a similar 32-kDa PMP in pea leaf peroxisomes by showing that this PMP had ferricyanide reductase activity and was recognized by antibodies raised against a cucumber MDAR. Interestingly, these same antibodies were shown very recently to recognize a 47-kDa castor polypeptide that was associated with MDAR enzymatic activity in alkaline carbonate washed glyoxysomal membranes (Karyotou and Donaldson, 2005).

Despite this biochemical evidence, a gene coding for a peroxisomal membrane-bound MDAR has yet to be identified and described. Genes coding for putative matrix peroxisomal MDAR polypeptides have been cloned from pea (Murthy and Zilinskas, 1994), cucumber (Sano and Asada, 1994), tomato (Grantz *et al.*, 1995) and Chinese cabbage (Yoon *et al.*, 2004), and databases include reports of similar cDNAs/genes in rice (GenBank accession number D85764), broccoli (AB125637), iceplant (AJ301553) and *Arabidopsis* (AGI Locus At3g52880). The primary amino acid sequences of all these predicted MDARs include a type 1 matrix peroxisomal targeting signal (PTS1) that consists of a C-terminal tripeptide that resembles the canonical -SKL motif (Mullen, 2002; Olsen and Harada, 1995). Curiously, none of these MDARs have been evaluated for subcellular localization, nor have any of their C-terminal sequences been shown to function as a PTS.

Nearly all peroxisomal proteins are synthesized on cytosolic polyribosomes and then post-translationally targeted to pre-existing and/or differentiating organelles. In addition to the PTS1 mentioned above, many PMPs are targeted to the peroxisomal membrane by a less well-characterized membrane PTS (mPTS) that consists of a hydrophobic transmembrane domain (TMD) and an adjacent cluster of basic amino acids (Dyer *et al.*, 1996; Hunt and Trelease, 2004; Jones *et al.*, 2001; Mullen and Trelease, 2000; Wang *et al.*,

2001). Coupled with the lack of secretory pathway targeting determinants, the presence of any PTS predicts that nascent matrix polypeptides or PMPs sort directly from their site of synthesis in the cytosol to peroxisomes. This direct pathway has been demonstrated for yeast PMP47 (Dyer *et al.*, 1996) and *Arabidopsis* peroxin 3 (Hunt and Trelease, 2004), both of which possess a mPTS. However, recent findings suggest that at least some PMPs follow an indirect sorting pathway that includes the endoplasmic reticulum (ER). For example, peroxisomal APX and *Arabidopsis* peroxin 16 appear in a subdomain(s) of rough ER before reaching the peroxisomal membrane in *Arabidopsis* and BY-2 cultured cells (Karnik and Trelease, 2005; Lisenbee *et al.*, 2003a,b; Mullen *et al.*, 1999, 2001). Considering the cooperative functional roles of MDAR and APX, it is interesting that intracellular sorting pathways have not been elucidated for any of the MDARs identified previously.

Our goal in the present study was to establish a much-needed link between the genetic and protein components responsible for peroxisomal MDAR activity in plants. Obara *et al.* (2002) predicted the existence of seven MDAR polypeptides in *Arabidopsis* from as many then-available gene and cDNA sequences. In that work, they characterized two of the polypeptides as chloroplast and mitochondrial isoforms that were coded from a single alternatively transcribed open reading frame (ORF). Subsequent sequence updates indicate that this ORF resides within one of five MDAR loci in *Arabidopsis*, from which only six MDAR polypeptides may be predicted (assuming no other instances of alternative gene regulation). Two of the four uncharacterized MDARs are predicted 47- and 54-kDa polypeptides that possess a PTS1 and an mPTS, respectively. We cloned all four uncharacterized *Arabidopsis* MDARs and found from *in vivo* immunofluorescence sorting and targeting analyses that both of the putative peroxisomal MDARs sorted directly to *Arabidopsis* and BY-2 suspension cell peroxisomes in a PTS-dependent manner. These protein products corresponded to endogenous 47- and 54-kDa *Arabidopsis* polypeptides that in biochemical assays were associated both structurally and functionally with the peroxisomal matrix and membrane, respectively. The details of these findings with respect to enzyme function, protein sorting, organelle association and topology now provide a more complete foundation upon which models of peroxisomal ascorbate metabolism may be tested.

Results

Identification of AtMDAR1 and AtMDAR4 as representative matrix- and membrane-localized peroxisomal MDARs

For the purposes of this study, *Arabidopsis* gene loci are referred to by their AGI names and the proteins by the given names AtMDAR1 to AtMDAR6. AtMDAR1 (At3g52880)

possesses a C-terminal -AKI tripeptide that resembles the PTS1 signal for directing proteins to the peroxisomal matrix. Similarly, AtMDAR4 (At3g27820) contains within a unique C-terminal extension mPTS-like sequences that comprise a predicted TMD followed immediately by five basic arginine residues. Neither AtMDAR2 (At5g03630) nor AtMDAR3 (At3g09940) include sequence features that predict specific subcellular (organellar) localizations. AtMDAR5 and AtMDAR6 (At1g63940) are the respective mitochondrial and chloroplast MDARs that have been characterized previously (Obara *et al.*, 2002).

We searched the literature and protein sequence databases for PTS-containing plant MDAR homologs with the goal of identifying sequences that would validate the predicted peroxisomal localizations and MDAR functions of AtMDAR1 and AtMDAR4. The results are listed in Table 1 and are arranged in ascending order according to mass. Most of the sequences corresponded to MDAR polypeptides that possessed a C-terminal PTS1 signal. All these sequences had predicted masses of approximately 47 kDa and possessed the NADP/FAD binding domains that are typical of flavoproteins such as MDAR that belong to the pyridine nucleotide-disulphide oxidoreductase family (Pfam accession number PF00070). In comparison, AtMDAR1 is at least 76% identical to any one of the seven other PTS1-containing MDARs listed

in Table 1 (alignment not shown). AtMDAR1 also contains three sequence motifs that correspond to the NADP/FAD binding domains typified by the cucumber and pea polypeptides, both of which have been purified and shown to exhibit NADH-dependent MDAR activity *in vitro* (Murthy and Zilinskas, 1994; Sano *et al.*, 1995). Furthermore, the C-terminal -AKI tripeptide of AtMDAR1 matches the PTS1-like motif -(S/A)K(I/V) (Mullen, 2002) that is shared among this group of 47-kDa MDARs. The presence of functional domains responsible for MDAR catalytic activity and for targeting to peroxisomes supports the assignment of AtMDAR1 as an authentic peroxisomal matrix MDAR.

The biochemical and sequence data compiled in Table 1 indicated the existence of at least one other group of peroxisomal MDARs. This group consisted of four predicted approximately 52–54 kDa polypeptides that contained putative TMD regions at both ends of the proteins. AtMDAR4 is 70% identical to any one of the other group members (alignment not shown), all of which possess the three NADP/FAD binding motifs of the 47-kDa cucumber MDAR that also were identified in AtMDAR1. The C-terminal-most TMD of AtMDAR4 is defined on each end by conserved proline and glycine residues and is situated adjacent to a tryptophan-capped basic cluster -R(K/R)RRR that is shared by all five polypeptides (including an incomplete sequence from

Table 1 Evidence for (putative) peroxisomal matrix and membrane MDAR proteins

Organism	Predicted size (kDa)	SDS-PAGE size (kDa)	(Predicted) location	GenBank no./AGI locus	Reference
<i>Pisum sativum</i>	n.d.	32 ^c	Membrane	n.a.	López-Huertas <i>et al.</i> (1999)
<i>Ricinus communis</i>	n.d.	32 ^d	Membrane	n.a.	Luster <i>et al.</i> (1988)
<i>Hordeum vulgare</i>	38.9 ^a	n.d.	Membrane	CAC69935	Unpublished
<i>Glycine max</i>	n.d.	39/40 ^e	Unknown	n.a.	Dalton <i>et al.</i> (1992)
<i>Arabidopsis thaliana</i>	46.5	47 ^f	Matrix	At3g52880	This study
<i>Brassica oleracea</i>	46.5	n.d.	Matrix	BAD14934	Unpublished
<i>Brassica campestris</i>	46.5	n.d.	Matrix	AAK72107	Yoon <i>et al.</i> (2004)
<i>Oryza sativa</i>	46.6	n.d.	Matrix	BAA77214	Unpublished
<i>Mesembryanthemum crystallinum</i>	47.0 ^b	n.d.	Matrix	CAC82727	Unpublished
<i>Lycopersicon esculentum</i>	47.0	n.d.	Matrix	AAC41654	Grantz <i>et al.</i> (1995)
<i>Ricinus communis</i>	n.d.	47 ^g	Membrane	n.a.	Karyotou and Donaldson (2005)
<i>Pisum sativum</i>	47.3	47 ^h	Matrix	AAA60979	Murthy and Zilinskas (1994); this study
<i>Cucumis sativus</i>	47.4	47 ^{i,j}	Matrix	BAA05408	Hossain and Asada (1985); Sano <i>et al.</i> (1995)
<i>Oryza sativa</i>	51.9	n.d.	Membrane	AAL87166	Unpublished
<i>Zea mays</i>	52.0	n.d.	Membrane	AY106646	Gardiner <i>et al.</i> (2004)
<i>Triticum aestivum</i>	52.2	n.d.	Membrane	BT009417	Unpublished
<i>Arabidopsis thaliana</i>	53.5	54 ^k	Membrane	At3g27820	This study

Publicly available literature and sequence databases were searched for data supporting the existence of MDAR-like gene(s) and protein(s) affiliated with the ascorbate metabolism of plant peroxisomes. Listed in ascending order according to size are only those candidates for which the available experimental and/or sequence data strongly support peroxisomal functions. For MDAR-like sequences that have yet to be verified experimentally, the criteria for inclusion were the presence of amino acid sequences that resembled matrix or membrane peroxisomal targeting signals. Predicted sizes of polypeptides were calculated with the SAPS algorithm (Brendel *et al.*, 1992); ^aincomplete sequence, ^bportion of sequence homologous to matrix MDAR proteins. SDS-PAGE sizes, as reported in the references listed, were derived from the following sources: ^cimmunoblot, *P. sativum* leaf PMPs; ^dprotein stain, *R. communis* glyoxysomal membrane extracts; ^eprotein stain, purified proteins from *G. max* root nodule extracts; ^fimmunoblot, *A. thaliana* suspension cell peroxisomal matrix fractions; ^gimmunoblot, *R. communis* glyoxysomal membrane fractions; ^hprotein stain, *E. coli* expressed proteins; ⁱprotein stain, purified proteins from *C. sativus* fruit extracts; ^jimmunoblot, *E. coli* expressed proteins; ^kimmunoblot, *A. thaliana* suspension cell peroxisomal membrane fractions. n.d., not determined; n.a., not available.

barley). Together the TMD and basic cluster form a C-terminal mPTS, neither component of which was found in any of the 47-kDa MDAR sequences. These comparisons suggest the classification of AtMDAR4 as an authentic peroxisomal membrane MDAR, and when combined with those of the 47-kDa group reveal the presence of two predominant MDAR isoforms in plant peroxisomes that in *Arabidopsis* are represented by AtMDAR1 and AtMDAR4.

Arabidopsis peroxisomes possess separate matrix and membrane MDARs

Sucrose density gradient separations were employed to assess the distributions of MDAR polypeptides and enzyme activities in subcellular fractions of *Arabidopsis* suspension cells. The representative gradient profiles shown in Figure 1(a) demonstrate that most of the peroxisomes

equilibrated in the 1.25 g ml⁻¹ regions of the gradients. These regions were well separated from mitochondria and were largely devoid of starch-containing non-green plastids that were removed from crude homogenates prior to gradient centrifugations (data not shown). Smaller peaks of catalase activity, marking either damaged peroxisomes and/or intact pre-peroxisomes, were measured consistently in the higher-density fractions of the mitochondrial regions. Relatively few peroxisomes were burst during the homogenization procedure, as evidenced by the low catalase activity in the soluble/cytosolic regions (fractions 24–29). These results are consistent with previous separations of *Arabidopsis* suspension cells, although the improved methods utilized here yielded three to seven times more catalase activity in the peroxisomal regions and reduced by at least 50% the catalase activity in the soluble regions (Flynn *et al.*, 2005; Lisenbee *et al.*, 2003a). Thus, via isopycnic centrifugation we were able to collect a high proportion of applied peroxisomes that were intact and virtually free of mitochondria and plastids.

MDAR activity exhibited three separate peaks in the peroxisomal, mitochondrial and cytosolic regions of the gradients (Figure 1a). The representative immunoblot analyses shown in Figure 1(b) indicate that these enzyme activities were attributable to MDAR polypeptides detected in peak peroxisomal, mitochondrial and cytosolic fractions. Specifically, peroxisomal fractions possessed two MDARs with apparent masses of 47 and 54 kDa, the latter being most abundant in fractions 5–7. Mitochondrial and cytosolic fractions also contained 47-kDa MDARs, as well as a 38-kDa MDAR in the cytosolic samples that was most prevalent in fractions 26 and 27. Most of these MDARs were detected in the clarified homogenates that were applied to the sucrose gradients, although the high protein concentration of these samples often precluded detection of the less-abundant MDARs, particularly the 54-kDa MDAR. Combined, the enzyme profiles and immunoblot analyses shown in Figure 1 demonstrate that peak MDAR activities equilibrate in well-separated peroxisomal, mitochondrial and cytosolic fractions of *Arabidopsis* suspension cells, each of which retains one or more different MDAR polypeptides.

Isolated peroxisomes were examined in more detailed enzymatic and biochemical analyses to determine if the endogenous 47- and 54-kDa MDAR polypeptides corresponded to any of the AtMDAR proteins that were predicted from *Arabidopsis* gene sequences. Table 2 lists enzyme activity data, and Figure 2(a) shows immunoblot analyses of MDAR and APX detected in peroxisomes and peroxisomal subfractions. Incubation of intact organelles (Figure 2a, lane 1) in hypotonic buffer and separation of membranes by centrifugation released portions of the 47-kDa MDAR into the water-soluble matrix (Figure 2a, lane 2) that exhibited three-quarters of the MDAR and catalase activities associated with peroxisomes (Table 2). This treatment did not release the

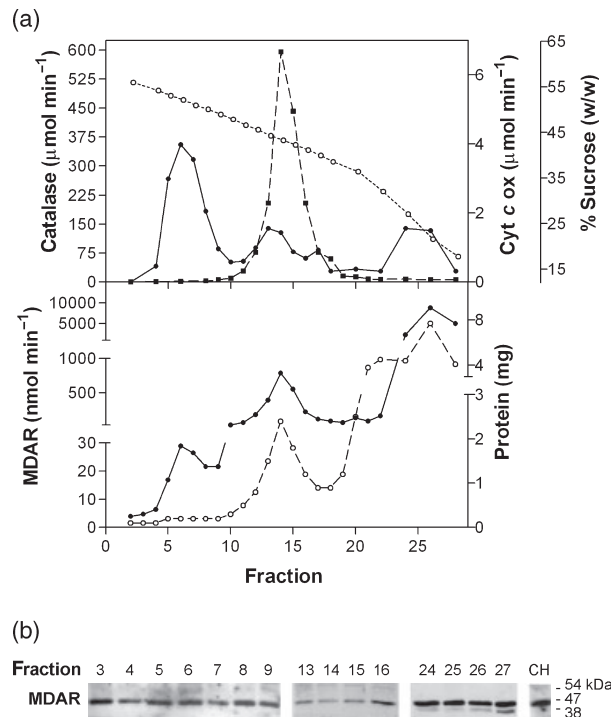


Figure 1. Sucrose density gradient separation of organelles from *Arabidopsis* suspension cells and immunoblot analyses of MDAR polypeptides in selected fractions.

(a) Representative profiles showing the distributions of enzyme activities and protein within typical 30–59% w/w sucrose gradients. In the upper panel, peroxisomal catalase activities (closed circles) demonstrate the consistent separation and high yield of intact peroxisomes from mitochondria (cytochrome *c* oxidase activity, closed squares); open circles denote the density of each fraction. The lower panel shows that peroxisomal, mitochondrial and soluble/cytosolic gradient fractions possessed separate peaks of MDAR enzyme activity (closed circles) and protein (open circles).

(b) Representative immunoblot analyses (25 µg protein per lane) showing the distribution of MDAR polypeptides in selected trichloroacetate-precipitated gradient fractions and clarified homogenate (CH). MDAR polypeptides were detected with a polyclonal antibody raised against a 47-kDa MDAR from *Cucumis sativus* fruits.

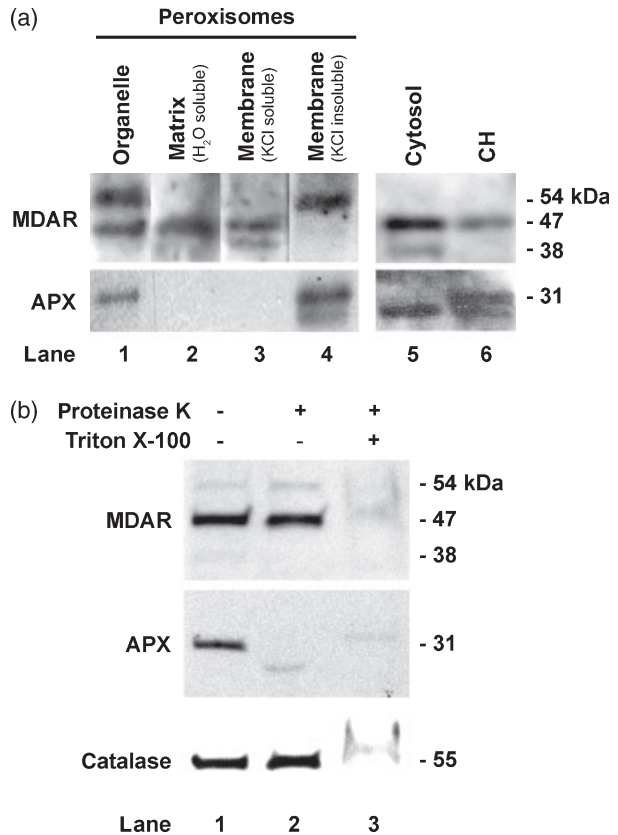
Table 2 Enzyme activity and amount of protein in subfractions of peroxisomes and mitochondria isolated in sucrose density gradients

	MDAR (nmol min ⁻¹)	Catalase (μ mol min ⁻¹)	Cytochrome <i>c</i> oxidase (μ mol min ⁻¹)	Protein (mg)
Applied sample ^a	33000	14700	20.5	120
Peroxisomes ^b	80.4	3500	0.12	1.50
Matrix	50.3	486	0	0.330
Membrane	14.9	119	0	0.300
KCl soluble	2.10	28.9	n.d.	0.040
KCl insoluble	11.7	80.6	n.d.	0.110
Mitochondria ^c	5500	189	47.3	17.1
Matrix	2010	115	0.165	6.20
Membrane	310	44.4	16.0	5.85
KCl soluble	200	50.0	0.01	0.93
KCl insoluble	350	0	14.0	4.30
Cytosol ^d	5380	583	0.24	39.1

Values are averages derived from two experiments. Each experiment utilized organelle fractions pooled from three separate sucrose gradients (e.g. Figure 1a): ^aclarified homogenate (1500 g supernatant, 15 min) applied to the top of each 30–59% w/w sucrose gradient in a vTi 50 rotor tube (8.4 ml split equally among three gradients); ^bfractions 4–8; ^cfractions 13–15; ^dfractions 25–28. n.d., not determined.

54-kDa MDAR or membrane-bound APX, and appreciable amounts of MDAR activity were found repeatedly in the resulting membrane pellets. Subsequent incubation of these membranes in KCl removed the remainder of the 47-kDa MDAR (Figure 2a, lane 3), but not the 54-kDa MDAR or APX, both of which remained associated with the KCl-insoluble pellet (Figure 2a, lane 4) that received nearly all the membrane-associated MDAR activity (Table 2). Cytosolic samples contained 38- and 47-kDa MDARs and the soluble form of APX (Figure 2a, lane 5) that were detected with other immunologically related proteins in the clarified homogenates (Figure 2a, lane 6). Mitochondria isolated from the same sucrose gradients exhibited 50 times more MDAR activity than peroxisomes, most of which was associated with the mitochondrial matrix, and not KCl-extracted membranes that exhibited cytochrome *c* oxidase activity (Table 2).

Intact peroxisomes also were incubated with proteinase K with or without Triton X-100 to elucidate the topological orientation of the endogenous Arabidopsis MDARs. As shown in Figure 2(b), all the MDAR polypeptides as well as APX and catalase remained unchanged in control reactions in which neither proteinase K or detergent was added (lane 1). Incubation of intact peroxisomes in protease alone (lane 2) resulted in the digestion of cytosolically oriented APX, but not the 47- and 54-kDa MDAR proteins or catalase. However, the latter three proteins were digested when the peroxisomes were treated first with Triton X-100 and then incubated in proteinase K (lane 3). Together, the *in vitro* results presented in Table 2 and Figure 2 show that Arabidopsis

**Figure 2.** Suborganellar distribution, membrane association, and topological orientation of MDAR polypeptides in Arabidopsis peroxisomes.

Proteins in Arabidopsis suspension cell peroxisomes (pooled from three sucrose gradients, e.g. Figure 1) and peroxisomal subfractions were precipitated in trichloroacetate, subjected to SDS-PAGE (50 μ g protein per lane), and then analyzed on blots for MDAR polypeptides that were detected with anti-cucurbit MDAR antibodies. Replicate immunoblots probed with anti-APX or anti-catalase IgGs provided positive controls for membrane- and matrix-localized proteins, respectively.

(a) Membrane association. Peroxisomes (lane 1) were subjected to hypotonic burst in 25 mM HEPES-KOH (pH 7.5) and centrifuged to produce water-solubilized protein supernatants (lane 2) and water-insoluble membrane pellets. Peripheral membrane proteins were extracted from these pellets in 0.2 M KCl and extracts were centrifuged to generate a KCl-soluble supernatant (lane 3) and KCl-insoluble pellet (lane 4). Cytosolic fractions (cleared of membranes by centrifugation, lane 5) and clarified homogenate (CH) (sample applied to the gradients, lane 6) also were examined.

(b) Membrane topology. Intact peroxisomes (lane 1) were treated with proteinase K without (-) and with (+) presolubilization in Triton X-100 (lanes 2 and 3, respectively).

peroxisomes retain two unique MDAR polypeptides that are distributed differentially among the membrane and matrix. More specifically, the 54-kDa MDAR is an integral membrane protein positioned on the matrix face of the membrane and, like catalase, the 47-kDa MDAR is in the matrix. These biochemical characteristics suggest that the endogenous 47- and 54-kDa peroxisomal MDARs are coded by the Arabidopsis genes *AtMDAR1* and *AtMDAR4*, respectively. Furthermore, the 47-kDa MDARs detected in mitochondria and the cytosol are probably coded by *AtMDAR5* and *AtMDAR2/3*.

AtMDAR1 sorts directly to peroxisomes by means of its PTS1 signal

The results of our sequence analyses matched those of our biochemical examinations in predicting the existence of separate 47- and 54-kDa polypeptides, namely *AtMDAR1* and *AtMDAR4*, which reside in the matrix and membrane of *Arabidopsis* peroxisomes. To confirm/refute these findings we cloned, epitope-tagged, and then overexpressed transiently *AtMDAR1*–*AtMDAR4* (Table 3) for *in vivo* localization in *Arabidopsis* and tobacco BY-2 suspension cells.

Figure 3(a–h) shows the results of *in vivo* sorting analyses of transiently expressed myc-*AtMDAR1*. After 5 h of transient gene expression, application of anti-myc primary and fluorophore-conjugated secondary antibodies revealed that nearly all the overexpressed myc-*AtMDAR1* was localized in the cytosol of either *Arabidopsis* (Figure 3a) or BY-2 (Figure 3c) cells. Curiously, after 20 h transgene expression most of the myc-*AtMDAR1* had localized in *Arabidopsis* cells to peroxisomes that also were marked with anti-catalase antibodies (Figure 3e,f). Similar results were obtained with BY-2 cells subjected to the same 20-h expression period (Figure 3g,h), although the relative amount of expressed myc-*AtMDAR1* localized to peroxisomes was much less than in *Arabidopsis* cells. Multiple labeling experiments with various organelle-specific markers were unable to detect myc-*AtMDAR1* in compartments other than the cytosol or peroxisomes, and allowing cells to express the transgenes for longer periods did not change the peroxisomal sorting seen at 20 h (data not shown). Partial localization to peroxisomes was not observed in experiments with myc-*AtMDAR2* (Figure 3i–l) or myc-*AtMDAR3* (Figure 3m–p), both of which were detected only in the cytosol in both cell types after 20 h expression. Cumulatively, these results demonstrate that *AtMDAR1* sorts directly to *Arabidopsis* and BY-2 cell peroxi-

somes, whereas *AtMDAR2* and *AtMDAR3* remain and probably function in the cytosol.

The sorting characteristics of *AtMDAR1* prompted us to analyze more closely the protein’s putative PTS1 tripeptide. Figure 4(a–d) shows that removal of the –AKI tripeptide from the C terminus of *AtMDAR1* (Table 3) abolishes its sorting to *Arabidopsis* and BY-2 cell peroxisomes after 20 h expression. This finding confirms the necessity of these three residues for peroxisomal targeting, and suggests that the analogous residues of the other seven 47-kDa MDARs listed in Table 1 also confer localization to peroxisomes. We tested this hypothesis with a partially characterized MDAR from pea and found that the results of similar *in vivo* sorting analyses mimicked those of *AtMDAR1*. More specifically, after 5 h expression nearly all the myc-PsMDAR was detected in the cytosol of *Arabidopsis* and BY-2 cells (Figure 4e–h), whereas after 20 h expression a portion of myc-PsMDAR was detected in peroxisomes (Figure 4i–l). We were able to increase the sorting efficiency of this MDAR, particularly in BY-2 cells, by changing the C-terminal tripeptide from-SKI to the more canonical-SKL. In both cell types, Figure 4(m–p) shows very little myc-PsMDAR (expressed for 20 h) in the cytosol and nearly perfect colocalization with endogenous catalase.

AtMDAR4 sorts directly to peroxisomal membranes and is inserted such that its N terminus is exposed to the cytosol

We also tested *in vivo* the hypothesis that transiently expressed myc-*AtMDAR4* sorts to peroxisomal membranes in *Arabidopsis* and BY-2 suspension cells. Figure 5(a–d) shows representative *Arabidopsis* (Figure 5a,b) and BY-2 (Figure 5c,d) cells expressing for 2.5 and 5 h, respectively, myc-*AtMDAR4* within peroxisomes that also contained the marker enzyme catalase. These periods were the earliest

Table 3 Alignment of C-terminal amino acid sequences of MDAR protein variants created for sorting and targeting experiments

MDAR variant name	C-terminal sequence
myc-<i>AtMDAR1</i>	-SFAAKI
myc- <i>AtMDAR1</i> -Δ3	-SFA
myc-PsMDAR	-SFASKI
myc-PsMDAR-I433L	-SFASKL
myc-<i>AtMDAR2</i>	-SFATNI
myc-<i>AtMDAR3</i>	-SFATKFYSTSL
myc-<i>AtMDAR4</i>	-GFAHTVVSQQKVEPKDIPSAEMVKQSASVVMIKKPLYVWHAATGVVVAASVAAFWFYGRRRRW
myc- <i>AtMDAR4</i> -Δ1	-GFAHTVVSQQKVEPKDIPSAEMVKQSASVVMIKKPLYVWHAATGVVVAASVAAFWFYGRRRR
myc- <i>AtMDAR4</i> -Δ6	-GFAHTVVSQQKVEPKDIPSAEMVKQSASVVMIKKPLYVWHAATGVVVAASVAAFWFY
myc- <i>AtMDAR4</i> -Δ38	-GFAHTVVSQQKVEPKDIPSAEMVKQSA
GFP- <i>AtMDAR4</i> (6)	-LYKSSRRRRRW
GFP- <i>AtMDAR4</i> (TMD)	-LYKSSVVMIKKPLYVWHAATGVVVAASVAAFWFY
GFP- <i>AtMDAR4</i> (38)	-LYKSSVVMIKKPLYVWHAATGVVVAASVAAFWFYGRRRRW

Epitope-tagged *A. thaliana* and *P. sativum* MDAR proteins (bold type) were aligned using the CLUSTALW algorithm. PTS1-like tripeptides are single-underlined. mPTS-like TMDs predicted with the TMHMM program (version 2.0) and basic (positively charged) amino acid clusters are bold type and double-underlined, respectively.

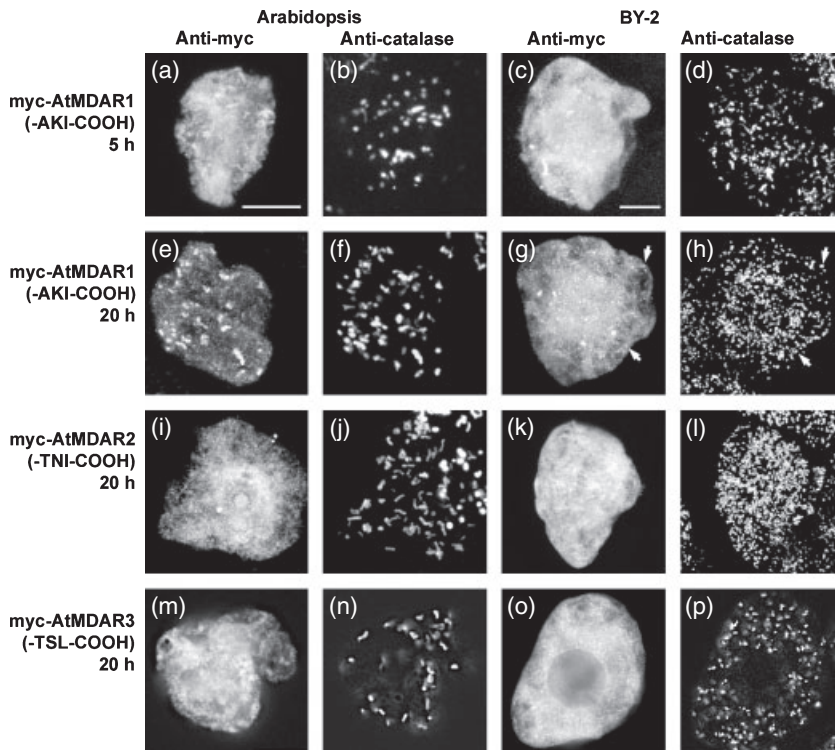


Figure 3. *In vivo* immunofluorescence sorting analyses of three Arabidopsis MDAR polypeptides expressed in Arabidopsis and BY-2 suspension cells.

Arabidopsis (a, b, e, f, i, j, m, n) and BY-2 (c, d, g, h, k, l, o, p) cells were bombarded with tungsten-bound genes coding for myc-epitope-tagged variants of AtMDAR1 (a–h), AtMDAR2 (i–l) or AtMDAR3 (m–p). Bombarded cells were allowed to express the transgenes for either 5 h (a–d) or 20 h (e–p) prior to formaldehyde fixation, Triton X-100 permeabilization and fluorescence co-immunolabeling for the expressed myc-tagged proteins (a, c, e, g, i, k, m, o) and endogenous peroxisomal catalase (b, d, f, h, j, l, n, p). Solid arrows in (g, h) indicate co-localizations of the two fluorescent markers within peroxisomes. All micrographs are confocal projection images. Bars in (a) and (c) = 10 μm and are the same for (b, e, f, i, j, m, n) and (d, g, h, k, l, o, p), respectively.

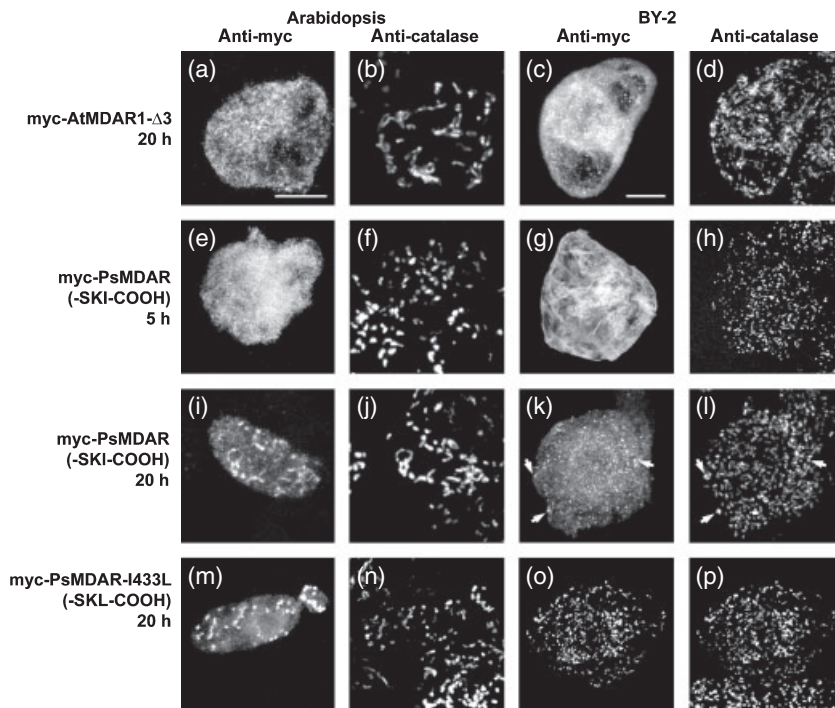


Figure 4. Necessity and efficacy of the PTS1-like C-terminal tripeptides of Arabidopsis and *Pisum sativum* approximately 47-kDa peroxisomal MDARs.

Arabidopsis (a, b, e, f, i, j, m, n) and BY-2 (c, d, g, h, k, l, o, p) cells expressing myc-epitope-tagged variants of AtMDAR1 or PsMDAR were fixed in formaldehyde, permeabilized with Triton X-100 and immunolabeled for the myc-tagged proteins (a, c, e, g, i, k, m, o) and endogenous peroxisomal catalase (b, d, f, h, j, l, n, p). (a–d) Cells expressing for 20 h myc-AtMDAR1-Δ3 which lacks the C-terminal PTS1 tripeptide –AKI. (e–h) Cells expressing for 5 h (e–h) or 20 h (i–l) myc-PsMDAR possessing the wild-type PTS1 tripeptide –SKI. (m–p) Cells expressing for 20 h myc-PsMDAR-I433L in which the C-terminal-most Ile residue was changed to Leu to create a canonical –SKL tripeptide. Solid arrows in (k, l) indicate colocalizations of the two fluorescent markers within peroxisomes. All micrographs are confocal projection images. Bars in (a) and (c) = 10 μm and are the same for (b, e, f, i, j, m, n) and (d, g, h, k, l, o, p), respectively.

time-points after which myc-AtMDAR4 could be detected reliably in these cells, and examinations of numerous images did not show the protein within any other organellar compartment. It should be noted that we observed overexpressed myc-AtMDAR4 within a non-peroxisomal

compartment in both cell types, although the effect was most pronounced in BY-2 cells after expression periods longer than 8 h (data not shown). A careful series of experiments confirmed that myc-AtMDAR4 had not sorted to ER or pER, and that the non-peroxisomal structures

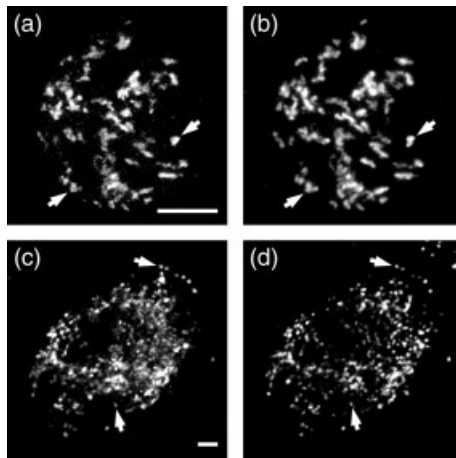


Figure 5. *In vivo* immunofluorescence sorting analyses of an Arabidopsis approximately 54-kDa MDAR polypeptide in Arabidopsis and BY-2 suspension cells. Arabidopsis (a, b) and BY-2 (c, d) cells bombarded with a gene coding for myc-AtMDAR4 were allowed to express the transgene for 2.5 and 5 h, respectively. Cells then were fixed in formaldehyde, permeabilized in Triton X-100 and co-immunolabeled with anti-myc (a, c) and anti-catalase (b, d) primary and fluorescence dye-conjugated secondary antibodies. Solid arrows point to examples of co-localization between the two fluorescent markers within catalase-containing peroxisomes. All micrographs are confocal projection images. Bars in (a, c) = 10 μ m.

instead represented an overexpression artifact that had been observed and described in detail previously (Lisenbee *et al.*, 2003b). Hence, our interpretation is that newly synthesized AtMDAR4 sorts in both cell types directly from the cytosol to peroxisomes, rather than indirectly to peroxisomes through pER.

Figure 6 summarizes the results of *in vivo* topology studies that utilized the N-terminal position of the myc epitope to elucidate the orientation of overexpressed myc-AtMDAR4. Arabidopsis cells bombarded with genes coding for myc-AtMDAR4 or myc-AtMDAR2 (control) were fixed in formaldehyde and then plasma membranes were permeabilized selectively with digitonin. In both cases, applied antibodies bound to exposed myc epitopes on the cytosolic surfaces of punctate peroxisomes for myc-AtMDAR4 (Figure 6a) or to epitopes distributed throughout the cytosol for myc-AtMDAR2 (Figure 6c). These labeling patterns resembled closely those of Triton X-100-permeabilized cells expressing myc-AtMDAR4 (Figure 5a) or myc-AtMDAR2 (Figure 3i). Dual labeling of the digitonin-permeabilized cells with anti-catalase antibodies confirmed the inaccessibility of antigens within the peroxisomal matrix (Figure 6b,d). In another control experiment, mock-transformed cells permeabilized with digitonin showed bright labeling of cytosolic microtubules (Figure 6e), whereas in the same cell endogenous catalase in the peroxisomal matrix was not accessible to applied IgGs (Figure 6f). From these experiments we conclude that the myc epitope of myc-AtMDAR4, and thus

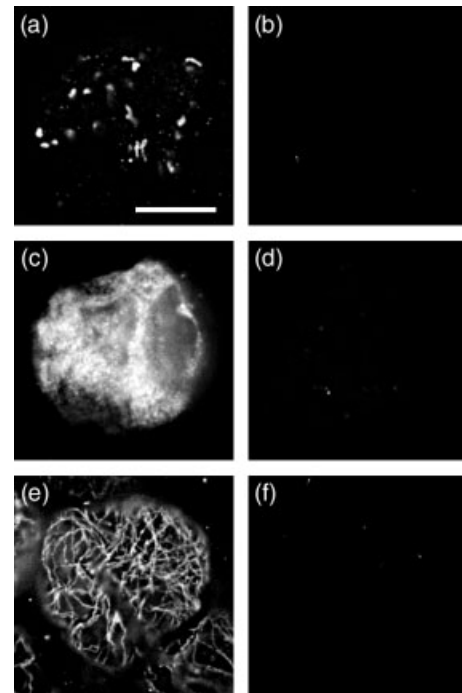


Figure 6. *In vivo* topological orientation of AtMDAR4 expressed in Arabidopsis cells. Cells bombarded with myc-AtMDAR4 or myc-AtMDAR2 were fixed in formaldehyde, perforated/digested with Pectinase and differentially permeabilized (plasma membranes only) with digitonin. (a–d) Transformed cells co-labeled with anti-myc antibodies for expressed myc-AtMDAR4 (a) or myc-AtMDAR2 (c) and with anti-catalase IgGs for endogenous peroxisomal catalase (b, d). (e, f) Representative mock-transformed cells colabeled for cytosolic microtubules (anti- α -tubulin antibodies) (e) and peroxisomal catalase (f). Bar in (a) = 10 μ m.

the N terminus of the AtMDAR4 polypeptide, is situated on the cytosolic face of peroxisomal membranes. Similar studies with BY-2 cells corroborated this orientation (data not shown).

The mPTS of AtMDAR4 is necessary and sufficient for targeting and insertion into peroxisomal membranes

A series of mutagenesis experiments was performed to determine whether the putative mPTS of myc-AtMDAR4 was responsible for the observed sorting to Arabidopsis and BY-2 peroxisomes. When we removed the C-terminal tryptophan of myc-tagged AtMDAR4 and expressed the mutant transiently in Arabidopsis cells, Figure 7(a,b) shows that the proteins were sorted normally to pre-existing peroxisomes that also contained matrix catalase. However, truncation of the tryptophan and the basic cluster (six C-terminal residues) eliminated completely targeting to peroxisomes (Figure 7c,d), as did removal of the entire putative mPTS (38 C-terminal residues) (Figure 7e,f). These Δ 6 and Δ 38 truncation mutants sorted instead to unidentified punctate (non-peroxisomal) structures and/or the cytosol, but not to

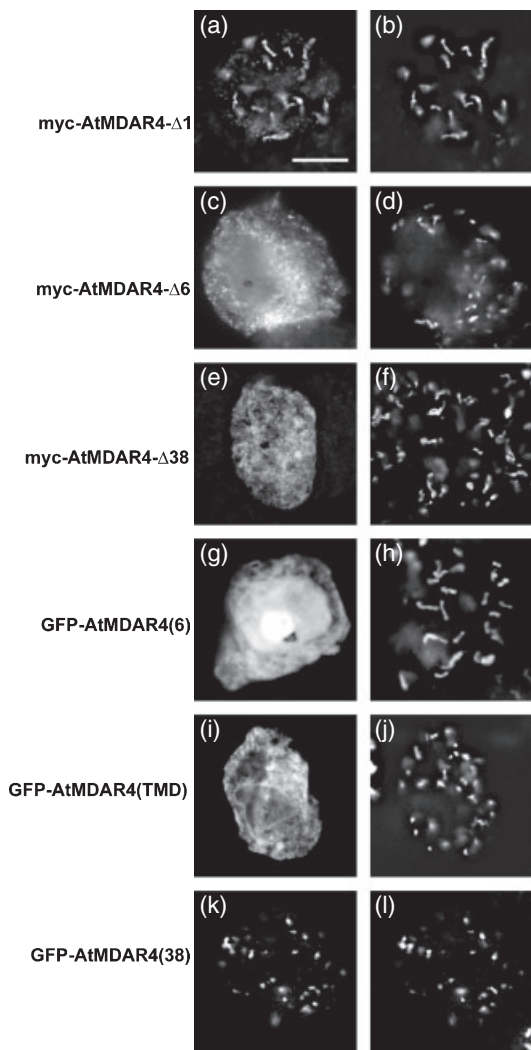


Figure 7. Necessity and sufficiency of the mPTS-like C-terminal 38 amino acid residues of AtMDAR4 for targeting to Arabidopsis suspension cell peroxisomes.

Arabidopsis cells were allowed to express for 5 h C-terminally truncated variants of myc-AtMDAR4 (a–f) or green fluorescent proteins (GFPs) appended with selected amino acid sequences of AtMDAR4 (g–l). Cells were fixed in formaldehyde, permeabilized with Triton X-100 and then (co-)immunolabeled as appropriate for the expressed myc-tagged proteins (a, c, e) and/or endogenous peroxisomal catalase (b, d, f, h, j, l). (a, b) Representative cell expressing myc-AtMDAR4- Δ 1 which was missing the single Trp residue at the C terminus. (c, d) Cell expressing myc-AtMDAR4- Δ 6 in which the six C-terminal-most amino acids, including the cluster of five basic Arg residues, had been removed. (e, f) Individual cell expressing myc-AtMDAR4- Δ 38 which had removed the entire mPTS-like peptide to include a predicted transmembrane domain (TMD) and the Arg cluster. (g, h) Individual cell expressing GFP-AtMDAR4(6) in which the six C-terminal-most amino acids of AtMDAR4 (including the basic cluster) were fused to the C terminus of GFP. (i, j) Representative cell expressing a GFP-AtMDAR4(TMD) variant that possessed at the C terminus of GFP amino acids constituting the predicted TMD within the C terminal tail of AtMDAR4. (k, l) Cell expressing a GFP-AtMDAR4(38) variant appended with the entire mPTS-like amino acid sequences of AtMDAR4. All micrographs are confocal projection images. Bar in (a) = 10 μ m.

fluorescent structures resembling reticular ER or circular aggregates of chloroplasts and mitochondria, as described in Lisenbee *et al.* (2003b).

In a separate set of experiments, C-terminal portions of AtMDAR4 were appended to a monomeric variant of green fluorescent protein (GFP) (Table 3) to ask which residues provide information sufficient for peroxisomal targeting. Figure 7(g,i) illustrates, respectively, that addition of either the basic cluster (six C-terminal residues) or the C-terminal TMD of AtMDAR4 to the C terminus of GFP did not permit targeting to catalase-containing peroxisomes in Arabidopsis cells (Figure 7h,j). Like the truncated myc-AtMDAR4 mutants, the majority of these GFP fusion proteins remained instead in the cytosol, with some in the nucleus (see Figure 7g). Conversely, when both the C-terminal TMD and the basic cluster (38 C-terminal residues) were appended to GFP, the expressed products targeted to Arabidopsis peroxisomes that also were marked by catalase (Figure 7k,l). From these findings, we conclude that the C-terminal TMD and basic cluster of AtMDAR4 together form an authentic mPTS that is both necessary and sufficient for peroxisomal targeting.

Discussion

Reduction of monodehydroascorbate is an important step in the recycling of the ascorbate antioxidants utilized by peroxisomes for turnover of potentially toxic H_2O_2 . Because direct recycling of monodehydroascorbate is performed by the NADH-dependent oxidoreductase MDAR, the ascorbate-mediated removal of reactive oxygen species has been linked to the secondary function of supplying the NAD needed for peroxisomal metabolism. However, recurring reports of peroxisomal MDAR activities and polypeptides from the past 20 years have yet to provide a set of results that have culminated in a general understanding of MDAR function(s) in peroxisomes. We have attempted to address this shortcoming with this comprehensive, multi-pronged analysis of previously uncharacterized MDAR gene and protein candidates in Arabidopsis.

The data compiled in Table 1 suggest that all but the most specialized plant peroxisomes require two different MDAR isoenzymes for proper regulation of ascorbate metabolism, grouped broadly as approximately 47-kDa matrix and approximately 54-kDa membrane polypeptides. Of the four uncharacterized Arabidopsis MDAR genes, only *AtMDAR1* and *AtMDAR4* code for MDAR polypeptides that could be assigned to these groups based upon structural features of the predicted proteins. Their high degree of amino acid identity to other well-characterized MDARs (Murthy and Zilinskas, 1994; Sano *et al.*, 1995), as well as our ability to detect MDAR activities and immunorelated 47- and 54-kDa polypeptides in isolated Arabidopsis peroxisomes, strongly support the assignment of *AtMDAR1* and *AtMDAR4* as bona fide NADH-dependent monodehydroascorbate reductases.

Coupled with the finding that epitope-tagged versions of AtMDAR1 and AtMDAR4 sorted to peroxisomes *in vivo*, we are confident that the *AtMDAR1* and *AtMDAR4* genes code for the *Arabidopsis* 47- and 54-kDa MDARs that appear to be common components of nearly all plant peroxisomes.

None of the four uncharacterized *Arabidopsis* MDARs appeared to represent the membrane-associated 32- and 47-kDa MDARs in castor glyoxysomal membranes, the 32-kDa MDAR in pea leaf peroxisomal membranes or the 39/40-kDa MDARs in soybean root nodule extracts (Table 1). Our biochemical results confirmed this notion by identifying 47- and 54-kDa MDAR polypeptides in isolated *Arabidopsis* peroxisomes, each of which exhibited distinguishable matrix and membrane associations, respectively, on blots that were probed with anti-cucumber 47-kDa MDAR antibodies (Sano *et al.*, 1995). These results were surprising, because the same antibodies recognized the seemingly very different 32-kDa pea and 47-kDa castor MDAR PMPs (Karyotou and Donaldson, 2005; López-Huertas *et al.*, 1999). In the current study, these antibodies also cross-reacted with a 38-kDa *Arabidopsis* polypeptide that was most abundant in cytosolic fractions. This polypeptide also was detected inconsistently in peroxisome preparations, and when present always behaved as a loosely attached, protease-sensitive component of intact organelles. These findings may point to the existence of as-yet unidentified peroxisomal MDARs in *Arabidopsis*, and to the speculation that the 38-kDa protein corresponds to the pea and castor 32-kDa MDARs and/or the soybean 39/40-kDa MDARs. Such a hypothesis is discredited by the fact that the 32-kDa MDARs exhibited much tighter associations with peroxisomal/glyoxysomal membranes than did the 38-kDa polypeptide (Bowditch and Donaldson, 1990; Jiménez *et al.*, 1997; López-Huertas *et al.*, 1999; Luster *et al.*, 1988). Although none of the *AtMDAR* genes coded for a 38-kDa polypeptide, another possibility is that the 47-kDa AtMDAR2 and/or AtMDAR3 isoforms that were shown in this study to remain in the cytosol are post-translationally processed to a cytosolic 38-kDa MDAR. Our contention is that the 38-kDa polypeptide is not another peroxisomal MDAR, but is instead an immunorelated cytosolic oxidoreductase that may associate peripherally with the cytosolic side of peroxisomal membranes, although the unreliable behavior of this interaction probably indicates that it was an artifact of the cell fractionations.

The inability of KCl to remove most of the 54-kDa polypeptide (AtMDAR4) and enzyme activity from peroxisomal membranes is consistent with previous results, and in our opinion provides the most reliable measure of membrane association in this system. For example, KCl treatments also did not remove MDAR enzyme activities from spinach glyoxysomal (Ishikawa *et al.*, 1998) or pea leaf peroxisomal (Jiménez *et al.*, 1997) membranes. In a more detailed analysis, Bowditch and Donaldson (1990) showed that KCl-treated castor glyoxysomal membranes retained

80% of the total pretreatment MDAR activity. Notably, this and another study (Bunkelmann and Trelease, 1996) also revealed that 0.1 M Na₂CO₃ abolished 85% of the total MDAR activity, prompting the authors to suggest that these conditions cannot be used to assess membrane associations. In support of this contention, our attempts at detecting MDAR polypeptides within peroxisomal membranes that had been extracted sequentially with KCl and then Na₂CO₃ yielded results that were inconsistent with those derived from use of KCl alone. Furthermore, these findings were not consistent with predictions of the biochemical behavior of matrix-associated catalase or the membrane association of an AtMDAR4 polypeptide having two putative TMDs. None the less, alkaline carbonate washes have been employed commonly in even the most recent studies of MDAR PMPs, but it must be emphasized that none of these studies have addressed the association of a 54-kDa MDAR. For instance, López-Huertas *et al.* (1999) showed that a 32-kDa pea leaf MDAR isolated from carbonate-washed peroxisomal membranes possessed NADH-dependent ferricyanide reductase activity; the MDAR activity of this polypeptide was not measured, due presumably to its carbonate inactivation. Karyotou and Donaldson (2005) detected MDAR activity in carbonate-washed castor glyoxysomal membranes, but this activity was attributed to a 47-kDa polypeptide that until this report had not been detected in castor. Considering our consistent immunodetection within KCl-washed peroxisomal membranes of a 54-kDa MDAR under conditions that preserved detectable MDAR activity, we conclude that AtMDAR4, like peroxisomal APX, is an integral membrane protein of *Arabidopsis* peroxisomes.

As predicted, the PTS sequences of both AtMDAR1 and AtMDAR4 provided the targeting information necessary for sorting transiently expressed, epitope-tagged versions of these proteins to *Arabidopsis* and BY-2 peroxisomes. However, we were surprised to find that the C-terminal -AKI and -SKI tripeptides of AtMDAR1 and PsMDAR, respectively, may have functioned inefficiently in peroxisomal targeting. Although this could have been due to overexpression from the CaMV 35S promoter, others have concluded from similar observations that residues outside the PTS1 signal function as accessory sequences that enable peroxisomal targeting by non-optimal PTS1 combinations (Bongcam *et al.*, 2000; Mullen, 2002; Mullen *et al.*, 1997a,b). We did not test this hypothesis directly for AtMDAR1 or PsMDAR, but did note enhanced peroxisomal sorting upon changing the -SKI tripeptide of PsMDAR to -SKL. Similarly, the TMD and the adjacent basic amino acid cluster at the C terminus of AtMDAR4 together, but not singly, were necessary and sufficient for targeting to peroxisomes. Mullen and Trelease (2000) arrived at a similar conclusion with respect to the analogous TMD and basic cluster of peroxisomal membrane APX. The sorting of several PMPs to peroxisomal membranes depends upon a basic amino acid cluster

(Baerends *et al.*, 2000; Brosius *et al.*, 2002; Dyer *et al.*, 1996; Elgersma *et al.*, 1997; Honsho and Fujiki, 2001; Hunt and Trelease, 2004; Kammerer *et al.*, 1998; Murphy *et al.*, 2003; Soukupova *et al.*, 1999), and in some cases sorting occurs indirectly through the ER when the basic cluster is juxtaposed with a TMD (Baerends *et al.*, 1996, 2000; Elgersma *et al.*, 1997; Mullen and Trelease, 2000). Interestingly, the mPTS of AtMDAR4 is contained within an approximately 60 amino acid C-terminal extension that is strikingly similar to the mPTS-containing C-terminal extensions of peroxisomal membrane-bound APXs (Jespersen *et al.*, 1997; Mullen and Trelease, 2000). When protein sequence databases were queried with the C-terminal extensions of either AtMDAR4 or cottonseed peroxisomal APX, other plant peroxisomal APXs and the 54-kDa MDARs were the only mPTS-containing sequences identified (data not shown). Despite their similar mPTSs, our early stage time-course results suggest that AtMDAR4 does not sort to peroxisomes indirectly through the pER subdomain that is utilized by peroxisomal APX (Lisenbee *et al.*, 2003a,b; Mullen *et al.*, 1999).

Results presented in the current study also suggest that AtMDAR4 is associated with and inserted into the peroxisomal membrane in a manner different from peroxisomal APX, an integral type II ($N_{\text{cytosol}}-C_{\text{matrix}}$) tail-anchored PMP (Mullen and Trelease, 2000). For instance, 54 kDa AtMDAR4 in intact peroxisomes was inaccessible to applied proteases in the absence of detergent, indicating that most of the polypeptide faces the peroxisomal matrix and not the cytosol. This 'reverse' orientation of AtMDAR4 places the enzyme's active site within the peroxisomal matrix, thus indicating that the PMP is by definition not a C-terminal tail-anchored protein with a large functional domain in the cytosol (Wattenberg and Lithgow, 2001). A separate set of topology experiments showed that the N terminus of AtMDAR4 was accessible to applied IgGs under conditions that prevented detection of matrix antigens. These data are consistent with the most accurate TMD algorithms that predict membrane-spanning regions at each end of the polypeptide (Möller *et al.*, 2001), as well as with the finding that the 54-kDa AtMDAR4 behaved as a KCl-insoluble, integral component of Arabidopsis peroxisomal membranes. This topology clearly carries functional implications for MDAR catalytic activity (see below), particularly in that the N-terminal TMD of AtMDAR4 curiously includes one of the FAD-binding sequence motifs that categorizes the protein in part as an authentic MDAR. None the less, it seems clear that upon reaching the peroxisomal membrane, newly synthesized AtMDAR1 is inserted into and resides within the matrix, whereas nascent AtMDAR4 is integrated, such that the bulk of the polypeptide is on the matrix face of the membrane with the N terminus exposed to the cytosol.

The diagram shown in Figure 8 incorporates the data presented in this study into a new understanding of the subcellular localizations and functional implications of the

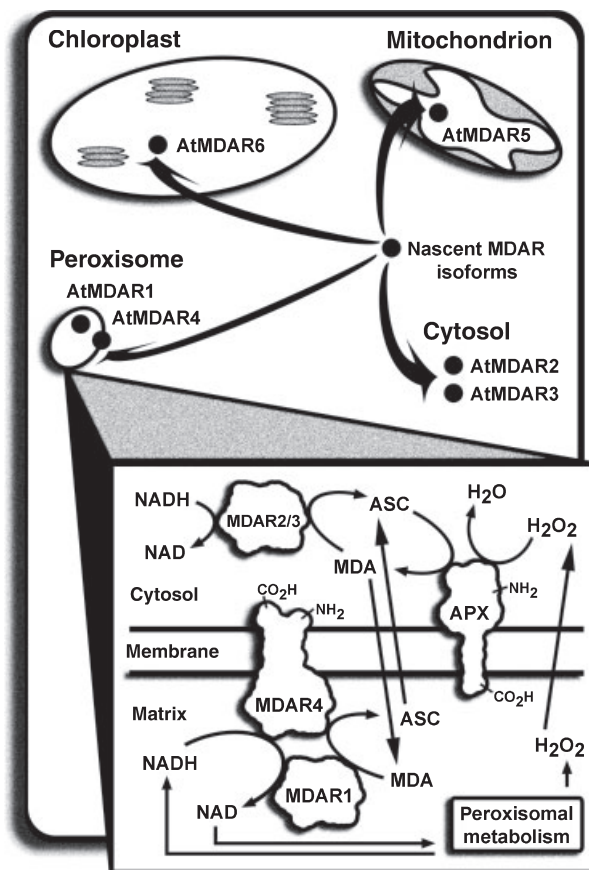


Figure 8. Model depicting the subcellular locations of MDAR isoforms in Arabidopsis cells and the potential functions of several MDARs in peroxisomal ascorbate recycling.

MDAR proteome in Arabidopsis. In the top portion of the figure, nascent MDAR polypeptides in the cytosol are sorted to known sites of ascorbate metabolism: AtMDAR1 and AtMDAR4 to the peroxisomal matrix and membrane, AtMDAR2 and AtMDAR3 to the cytosol and AtMDAR5 and AtMDAR6 to the mitochondrial matrix and chloroplast stroma, respectively (Obara *et al.*, 2002). In peroxisomes, monodehydroascorbate reduction is coordinated among cytosolic and peroxisomal MDARs on both sides of the peroxisomal membrane (Figure 8, inset), and probably occurs in concert with its production by the cytosolically oriented peroxisomal APX. That the active site of Arabidopsis peroxisomal APX is on the cytosolic face of the membrane (Lisenbee *et al.*, 2003a) suggests oxidized ascorbate is produced in the cytosol and is thus inaccessible to the matrix-localized active sites of the two peroxisomal MDARs. It may be reasonable to predict, however, that some or all of the substrates required by APX and MDAR permeate the peroxisomal membrane. Peroxisomes have been shown to be permeable to H₂O₂, and substrate shuttles have been documented in conjunction with several metabolic pathways (Donaldson, 2002). The depictions in Figure 8 also agree with

the reported matrix-associated MDAR activities of pea leaf peroxisomes (Jiménez *et al.*, 1997) and castor glyoxysomes (Bowditch and Donaldson, 1990), but it is notable that these studies did not determine whether the activities originated from a matrix protein and/or a PMP. In contrast, enzyme latency studies showed that the active sites of spinach peroxisomal MDAR were on the cytosolic side of the membrane (Ishikawa *et al.*, 1998). Donaldson (2002) has provided the particularly relevant explanation that these observations in spinach may represent a matrix-facing enzyme whose substrates permeate the membrane at rates greater than the enzyme's turnover number. More recent work from this group also suggested that APX and MDAR form a cooperative membrane-bound complex for the efficient removal of H₂O₂ (Karyotou and Donaldson, 2005), possibly to effect the direct shuttling of substrates and electron equivalents across the peroxisomal membrane. Regardless of the exact mechanism, this new representation provides the most complete and detailed understanding to date of how APX and MDAR might be configured functionally within the peroxisomal matrix and membrane for the removal of reactive oxygen species.

Experimental procedures

Arabidopsis cell culture, sucrose gradient isolation and subfractionation of organelles, enzyme assays and membrane protein association and topology

Arabidopsis (*Arabidopsis thaliana* var. Landsberg *erecta*) suspension cells (50 ml cultures) were grown, maintained and harvested according to Lisenbee *et al.* (2003a). For isolation of organelles in sucrose gradients, protoplasts were prepared prior to cell disruption as follows. Cells collected by centrifugation from each 4-day culture were washed twice (5 min each at room temperature) with 25 ml of aqueous 0.4 M D-mannitol. The cells were then resuspended in 25 ml of protoplasting solution [*Arabidopsis* culture medium (Lisenbee *et al.*, 2003a) plus 0.4 M D-mannitol, 0.1% w/v Pectinase (Sigma-Aldrich, St Louis, MO, USA) and 1% w/v Cellulase Y-C (Karlhan Research Products, Cottonwood, AZ, USA)] and incubated with rocking inversion at 30°C until the 20–30-cell clusters typical of *Arabidopsis* suspension cultures were reduced to one to four cells per cluster (approximately 2.5 h). The protoplasts were pelleted in a fixed-angle Sorvall SS-34 rotor at 480 *g* for 10 min and washed subsequently three times in aqueous 0.4 M D-mannitol before final resuspension in two pellet volumes of ice-cold homogenization medium (HM) (25 mM HEPES-KOH, pH 7.5, 0.7 M sucrose, 3 mM dithiothreitol (DTT) and 0.5 mM phenylmethylsulfonyl fluoride).

Resuspended cells (5–6 ml, equivalent to 1–1.5 flasks of 4-day cells) were disrupted with an ice-cold 15-ml Dounce (Wheaton Science Products, Millville, NJ, USA) tissue grinder (pestle 'A') using 25–35 up-and-down movements until approximately 80% of the cells were ruptured as judged by optical microscopy. Homogenates were centrifuged in a Sorvall HB-6 swing-out rotor at 1500 *g* for 15 min at 4°C to pellet unbroken cells, starch-containing non-green plastids, nuclei and cell debris. The resulting supernatants (2.5–3 ml, equivalent to 1 flask of 4-day cells) were loaded onto 25-ml linear gradients (30–59% w/w sucrose in 25 mM HEPES-KOH, pH

7.5) underlaid with 5-ml cushions (59% w/w sucrose) in Beckman vTi 50 Quick-Seal centrifuge tubes (Beckman Coulter, Fullerton, CA, USA). Each applied sample was overlaid with HM (0.4 M sucrose) before the gradient tubes were heat-sealed and then centrifuged in a vTi 50 rotor at 50 000 *g* for 75 min at 4°C. Peroxisomes equilibrated as a white band near the bottom of the gradients clearly separated from the larger mitochondrial band at lower sucrose density. Fractions (1 ml) were collected by hand through a hole punctured in the bottom of the tubes. The peroxisomes used for the topological studies presented in Figure 2(b) were isolated similarly according to the procedure detailed in Lisenbee *et al.* (2003a).

Experiments designed to elucidate the organellar distribution and membrane association of MDAR proteins in *Arabidopsis* peroxisomes were conducted mainly as described by Lisenbee *et al.* (2003a). The following describes important detailed differences. Organelles (Figure 1) in fractions 4–8 (peroxisomes), 13–15 (mitochondria) and 25–28 (cytosol) were pooled from each of three gradients. A duplicate set of pooled fractions from three other combined gradients also was prepared. Pooled peroxisomes (approximately 10 ml) or mitochondria (approximately 10 ml) were burst in 1.5 volumes of 25 mM HEPES-KOH, pH 7.5, with incubation (inversion rocking) for 40 min at 4°C. The suspensions were centrifuged in a Beckman fixed-angle 70 Ti rotor at 150 000 *g* for 45 min at 4°C to produce pelleted membranes and supernatants (water-solubilized proteins). The membrane pellets were resuspended in 1 ml (peroxisomes) or 4 ml (mitochondria) of 0.2 M KCl in 25 mM HEPES-KOH, pH 7.5, and incubated with intermittent mixing for 60 min at 4°C. KCl-insoluble membranes were pelleted from these suspensions in a Beckman 90 Ti rotor at 150 000 *g* for 30 min, generating a supernatant with KCl-soluble proteins. The KCl-insoluble membrane pellets were resuspended in 1 ml (peroxisomes) or 2 ml (mitochondria) of 0.2 M KCl in 25 mM HEPES-KOH, pH 7.5, for enzyme and protein assays. Peroxisomes used for protease-digestion (proteinase K) topology experiments were treated as described in detail in Lisenbee *et al.* (2003a).

Catalase and cytochrome *c* oxidase activities were assayed as described by Ni *et al.* (1990) and Tolbert *et al.* (1968), respectively. MDAR enzyme activities were assayed essentially as described by Bunkelmann and Trelease (1996). Briefly, the reaction was carried out in a final 1-ml volume of 50 mM HEPES-KOH, pH 7.6, 2.5 mM ascorbate (Sigma), 0.5 units ascorbate oxidase (Sigma), 5–100 μ l sample (up to 400 μ l in very dilute samples) and 0.1 mM NADH (Sigma). The components were added sequentially to a quartz cuvette and the linear decrease in A₃₄₀ was monitored for 1–2 min. These assays included measuring the potential rate of MDAR-independent NADH oxidation by omitting additions of ascorbate and ascorbate oxidase and subtracting this potential activity from the rate of MDAR-dependent NADH oxidation. Activity of the commercially supplied ascorbate oxidase was verified using a modification of the manufacturer's suggested assay, i.e., the decrease in A₂₆₅ of ascorbate was followed in a 1-ml reaction containing 50 mM HEPES-KOH, pH 7.6, ascorbate (A₂₆₅ approximately 0.907) and 0.5 units ascorbate oxidase.

Buoyant density measurement of sucrose gradient fractions, protein estimation, trichloroacetic acid (TCA) precipitation, sodium dodecyl sulphate-polyacrylamide gel electrophoresis (SDS-PAGE) and immunoblot detection were carried out essentially as described by Lisenbee *et al.* (2003a). The modifications used in this paper are that a final concentration of 0.05% w/v deoxycholate was added to all fractions prior to protein precipitation at a final concentration of 10% v/v TCA for 30 min at 4°C. Samples (25 μ g protein) were neutralized with solid Tris base and stored at 4°C as described. Samples were reduced by additions of freshly prepared 0.5 M or 1 M DTT to a final concentration of 10 mM, and then boiled 8 min prior to

separation in 10% w/v precast Mini-Protean II polyacrylamide gels (Bio-Rad, Hercules, CA, USA). Electrophoresis was performed for 45 min (for two gels). Primary and secondary antibodies were used as follows: rabbit anti-cucurbit 47-kDa MDAR antiserum (1:1000) (Sano *et al.*, 1995), rabbit anti-cucurbit peroxisomal APX IgGs (1:1000) (Corpas *et al.*, 1994), rabbit anti-cottonseed catalase IgGs (1:1000 or 1:2000) (Kunce *et al.*, 1988) and goat anti-rabbit alkaline phosphatase conjugate (1:10 000) (Bio-Rad).

Acquisition, subcloning and mutagenesis of MDAR coding sequences

Molecular biology reagents employed in standard recombinant DNA manipulations were purchased from Promega (Madison, WI, USA), New England Biolabs (Beverly, MA, USA) and Takara Biochemicals (Otsu, Shiga, Japan). Mutations were incorporated into coding sequences in polymerase chain reaction (PCR)-based site-directed mutagenesis reactions that included appropriate forward and reverse mutagenic primers. Mutagenic primer sets were designed for either fragment-specific or whole-plasmid PCR amplifications; the latter were carried out using the QuikChange site-directed mutagenesis kit according to the manufacturer's instructions (Stratagene, La Jolla, CA, USA). Custom oligonucleotide primers were synthesized by Genetech Biosciences (Tempe, AZ, USA), and all (mutated) plasmid inserts were confirmed by automated dye-terminator cycle sequencing (Arizona State University DNA Laboratory, Tempe, AZ, USA). Sequence details and DNA samples of all primer sets and plasmids used/created in this study are available from the authors upon request.

Full-length expressed sequence tag cDNAs were obtained from the Arabidopsis Biological Resource Center (Ohio State University, Columbus, OH, USA) for *A. thaliana* ecotype Columbia genes *AtMDAR1* (ABRC stock number U12996), *AtMDAR2* (U14648) and *AtMDAR3* (U21865). All three cDNAs were epitope-tagged as follows. First, open reading frames (ORFs) were amplified from their parent plasmids in PCR reactions that replaced start codons with in-frame *Bam*HI sites and appended *Xba*I sites after the stop codons. PCR products were TA cloned into pCR2.1 (Invitrogen, San Diego, CA, USA), digested with *Bam*HI and *Xba*I, and then ligated into *Bam*HI/*Xba*I-digested pRTL2/mycBX to yield pRTL2/myc-AtMDAR1, pRTL2/myc-AtMDAR2 and pRTL2/myc-AtMDAR3. pRTL2/mycBX is a CaMV 35S promoter-driven plant expression cassette that adds a single copy of the myc epitope to the 5' end of an ORF. The PsMDAR ORF was amplified from pSK/PsMDAR (Murthy and Zilinskas, 1994) and myc epitope-tagged as described above for AtMDAR1, except that the start codon was replaced with an *Xba*I-compatible *Nhe*I site for subcloning into an analogous pRTL2/mycX plant expression cassette. A full-length cDNA of *AtMDAR4* was amplified from 4-day Arabidopsis suspension cell total RNA using an RNeasy Plant Mini Kit (Qiagen, Valencia, CA, USA) and the access reverse transcription-polymerase chain reaction (RT-PCR) system (Promega), both according to the manufacturer's instructions. The forward primer corresponded to sequences downstream of the initiation codon, which was replaced by an in-frame *Nhe*I site. The reverse primer corresponded to sequences upstream of and including the termination codon and introduced a unique *Xba*I site within the 3' untranslated region. The cDNA products were TA cloned, sequenced to verify amplification of the correct MDAR ORF, and then subcloned into *Xba*I-digested pRTL2/mycX to yield epitope-tagged pRTL2/myc-AtMDAR4.

Sequences coding for the C-terminal PTS signals of AtMDAR1, PsMDAR and AtMDAR4 were modified for targeting necessity experiments as follows. pRTL2/myc-AtMDAR1-Δ3 was created from

pRTL2/myc-AtMDAR1 in a whole-plasmid PCR reaction that changed the GCT codon encoding A432 to a TGA stop codon. Similarly, pRTL2/myc-PsMDAR-I433L was created from pRTL2/myc-PsMDAR using complementary primers that changed the ATT codon encoding I433 to a leucine-coding TTA codon. To create pRTL2/myc-AtMDAR4-Δ1, the AtMDAR4 ORF was PCR-amplified from pRTL2/myc-AtMDAR4 using the forward primer described above and a mutagenic reverse primer that changed the final tryptophan-coding TGG codon to a TGA stop codon. The PCR products were TA cloned, digested with the appropriate restriction enzymes, and then ligated into pRTL2/mycX to yield pRTL2/myc-AtMDAR4-Δ1. Whole-plasmid PCR reactions were used to generate pRTL2/myc-AtMDAR4-Δ6 and pRTL2/myc-AtMDAR4-Δ38 from pRTL2/myc-AtMDAR4 with complementary primers that substituted TGA stop codons for those encoding amino acids R483 and S451, respectively.

Fusion of various portions of the mPTS of AtMDAR4 to the C terminus of GFP for targeting sufficiency experiments was accomplished as follows. pRTL2/GFP-AtMDAR4(6) was made by first annealing complementary oligonucleotides containing sequences coding for the RRRRRW basic cluster (six C-terminal residues) and stop codon of AtMDAR4. The resulting double-stranded fragments were phosphorylated with T4 polynucleotide kinase (New England Biolabs) and then ligated through designed 5' *Nhe*I and 3' *Xba*I overhangs into an *Xba*I-digested pRTL2/GFPX fusion cassette to yield pRTL2/GFP-AtMDAR4(6). pRTL2/GFPX was created from sequential whole-plasmid PCR reactions that inserted both an in-frame *Xba*I site in place of the stop codon and a monomer-inducing A206K mutation (Lisenbee *et al.*, 2003b; Zacharias *et al.*, 2002) into a plant optimized S65T variant of GFP (Haseloff *et al.*, 1997). pRTL2/GFP-AtMDAR4(TMD) and pRTL2/GFP-AtMDAR4(38) were made by first PCR-amplifying from pRTL2/myc-AtMDAR4 the TMD (residues 451–482) or the entire mPTS (residues 451–488) of AtMDAR4. Both reactions included a mutagenic forward primer that introduced an in-frame *Nhe*I site after the codon encoding amino acid A450; mutagenic reverse primers either substituted a TGA stop codon and an *Xba*I site for that encoding R483 [pRTL2/GFP-AtMDAR4(TMD)] or appended an *Xba*I site after the natural stop codon [pRTL2/GFP-AtMDAR4(38)]. TA-cloned PCR products were digested with the appropriate restriction enzymes and then ligated into *Xba*I-digested pRTL2/GFPX as described above.

BY-2 cell culture and microprojectile bombardment of suspension cells

Detailed descriptions of how *Nicotiana tabacum* L., cv. Bright Yellow 2 (BY-2) suspension-cultured cells were propagated in MS medium and how Arabidopsis and BY-2 cells were transformed via microprojectile bombardments can be found in Lisenbee *et al.* (2003a) and Mullen *et al.* (1999), respectively. For transient transformations, cells were resuspended in the appropriate transformation medium (MS medium without growth hormones), spread onto filter papers in petri dishes pre-wetted with the same medium and equilibrated for 1 h at room temperature in the dark. Equilibrated cells were bombarded with DNA-coated tungsten particles and then held in covered petri dishes for 2–20 h (sometimes longer) to allow for expression of the introduced transgene(s).

Immunofluorescence microscopy

Bombarded cells were scraped from filter papers, fixed in 4% w/v formaldehyde (prepared fresh from paraformaldehyde) (Ted Pella, Redding, CA, USA), and then perforated/digested in 0.1% w/v Pectolyase Y-23 (Karlan) and 0.1% w/v Cellulase RS (Arabidopsis only)

(Karlan) in preparation for immunofluorescence localization of the expressed proteins (Mullen *et al.*, 2001). Fixed and perforated cells were immunolabeled according to our standard 1-ml volume procedure described in Lisenbee *et al.* (2003a). Briefly, cells were permeabilized first in 0.3% v/v Triton X-100 (Sigma) and were then incubated for 1 h each in primary and fluorophore-conjugated secondary antibodies diluted in PBS. In experiments aimed at determining the topological orientation of proteins *in vivo* (Figure 6), *Arabidopsis* cells instead were perforated/digested in 0.1% w/v Pectinase for 1 h at 30°C and then were permeabilized selectively at plasma, but not organellar, membranes with 25 µg ml⁻¹ digitonin for 15 min at room temperature (Mullen *et al.*, 2001). Primary antibody sources and concentrations were as follows: mouse anti-myc monoclonal antibody 9E10 (1:500) (Santa Cruz Biotechnology, Santa Cruz, CA, USA), mouse anti-chick brain α -tubulin monoclonal antibody DM1A (1:500) (Accurate Chemical and Scientific Corp., Westbury, NY, USA) and rabbit anti-cottonseed catalase IgGs (1:500 or 1:2000) (Kunce *et al.*, 1988). Secondary immunoreagents conjugated to various green, red or far-red fluorophores were purchased from Jackson ImmunoResearch Laboratories (Westgrove, PA, USA). Immunolabeled cells were examined and photographed as described (Hunt and Trelease, 2004), and the resulting micrographs were adjusted for contrast and assembled into plates with Adobe Photoshop software (Adobe Systems, San Jose, CA, USA).

Acknowledgements

Thanks are extended to Satoshi Sano (Kyoto Prefectural University) for donating ample supplies of anti-cucumber MDAR antibodies and to Barbara Zilinskas (Rutgers University) for providing the PsMDAR cDNA clone. We also thank Robert Mullen (Guelph University) for constructing the pRTL2/mycX and pRTL2/mycBX cassettes and Scott Bingham (Arizona State University) for DNA sequencing and helpful advice on cloning techniques and procedures. Special thanks also are given to Sheetal Karnik for her helpful instructions and discussions pertaining to cell fractionation and biochemical techniques. Heather Gustafson (Arizona State University) maintained the suspension cultures and assisted in cell fractionations. Confocal microscopy was performed in the W.M. Keck Biolmaging Laboratory at Arizona State University. This work was supported by the National Science Foundation (grant no. MCB-0091826 to RNT) and in part by the William N. and Myriam Pennington Foundation. The Graduate Program in Molecular and Cellular Biology at Arizona State University funded a Research Assistantship for CSL.

References

- Baerends, R.J.S., Rasmussen, S.W., Hilbrands, R.E., van der Heide, M., Faber, K.N., Reuvekamp, P.T.W., Kiel, J.A.K.W., Cregg, J.M., van der Klei, I.J. and Veenhuis, M. (1996) The *Hansenula polymorpha* PER9 gene encodes a peroxisomal membrane protein essential for peroxisome assembly and integrity. *J. Biol. Chem.* **271**, 8887–8894.
- Baerends, R.J.S., Faber, K.N., Kram, A.M., Kiel, J.A.K.W., van der Klei, I.J. and Veenhuis, M. (2000) A stretch of positively charged amino acids at the N terminus of *Hansenula polymorpha* Pex3p is involved in incorporation of the protein into the peroxisomal membrane. *J. Biol. Chem.* **275**, 9986–9995.
- Bongcam, V., Petétot, J.M., Mittendorf, V., Robertson, E.J., Leech, R.M., Qin, Y.-M., Hiltunen, J.K. and Poirier, Y. (2000) Importance of sequences adjacent to the terminal tripeptide in the import of a peroxisomal *Candida tropicalis* protein in plant peroxisomes. *Planta*, **211**, 150–157.
- Bowditch, M.I. and Donaldson, R.P. (1990) Ascorbate free-radical reduction by glyoxysomal membranes. *Plant Physiol.* **94**, 531–537.
- Brendel, V., Bucher, P., Nourbakhsh, I.R., Blaisdell, B.E. and Karlin, S. (1992) Methods and algorithms for statistical analysis of protein sequences. *Proc. Natl Acad. Sci. USA*, **89**, 2002–2006.
- Brosius, U., Dehmel, T. and Gärtner, J. (2002) Two different targeting signals direct human peroxisomal membrane protein 22 to peroxisomes. *J. Biol. Chem.* **277**, 774–784.
- Bunkelmann, J.R. and Trelease, R.N. (1996) Ascorbate peroxidase: a prominent membrane protein in oilseed glyoxysomes. *Plant Physiol.* **110**, 589–598.
- Corpas, F.J., Bunkelmann, J. and Trelease, R.N. (1994) Identification and immunochemical characterization of a family of peroxisome membrane proteins (PMPs) in oilseed glyoxysomes. *Eur. J. Cell Biol.* **65**, 280–290.
- Corpas, F.J., Barroso, J.B. and del Río, L.A. (2001) Peroxisomes as a source of reactive oxygen species and nitric oxide signal molecules in plant cells. *Trends Plant Sci.* **6**, 145–150.
- Dalton, D.A., Langeberg, L. and Robbins, M. (1992) Purification and characterization of monodehydroascorbate reductase from soybean root nodules. *Arch. Biochem. Biophys.* **292**, 281–286.
- Donaldson, R.P. (2002) Peroxisomal membrane enzymes. In *Plant Peroxisomes* (Baker, A. and Graham, I., eds). Dordrecht: Kluwer Academic Publishers, pp. 259–278.
- Dyer, J.M., McNew, J.A. and Goodman, J.M. (1996) The sorting sequence of the peroxisomal integral membrane protein PMP47 is contained within a short hydrophilic loop. *J. Cell Biol.* **133**, 269–280.
- Elgersma, Y., Kwast, L., van den Berg, M., Snyder, W.B., Distel, B., Subramani, S. and Tabak, H.F. (1997) Overexpression of Pex15p, a phosphorylated peroxisomal integral membrane protein required for peroxisome assembly in *S. cerevisiae*, causes proliferation of the endoplasmic reticulum membrane. *EMBO J.* **16**, 7326–7341.
- Flynn, C.R., Heinze, M., Schumann, U., Gietl, C. and Trelease, R.N. (2005) Compartmentalization of the plant peroxin, AtPex10p, within subdomain(s) of ER. *Plant Sci.* **168**, 635–652.
- Gardiner, J., Schroeder, S., Polacco, M.L. *et al.* (2004) Anchoring 9371 maize expressed sequence tagged unigenes to the bacterial artificial chromosome contig map by two-dimensional overgo hybridization. *Plant Physiol.* **134**, 1317–1326.
- Grantz, A.A., Brummell, D.A. and Bennett, A.B. (1995) Ascorbate free radical reductase mRNA levels are induced by wounding. *Plant Physiol.* **108**, 411–418.
- Haseloff, J., Siemering, K.R., Prasher, D.C. and Hodge, S. (1997) Removal of a cryptic intron and subcellular localization of green fluorescent protein are required to mark transgenic *Arabidopsis* plants brightly. *Proc. Natl Acad. Sci. USA*, **94**, 2122–2127.
- Honsho, M. and Fujiki, Y. (2001) Topogenesis of peroxisomal membrane protein requires a short, positively charged intervening-loop sequence and flanking hydrophobic segments. Study using human membrane protein PMP34. *J. Biol. Chem.* **276**, 9375–9382.
- Hossain, M.A. and Asada, K. (1985) Monodehydroascorbate reductase from cucumber is a flavin adenine dinucleotide enzyme. *J. Biol. Chem.* **260**, 12920–12926.
- Hunt, J.E. and Trelease, R.N. (2004) Sorting pathway and molecular targeting signals for the *Arabidopsis* peroxin 3. *Biochem. Biophys. Res. Commun.* **314**, 586–596.
- Ishikawa, T., Yoshimura, K., Sakai, K., Tamoi, M., Takeda, T. and Shigeoka, S. (1998) Molecular characterization and physiological

- role of a glyoxysome-bound ascorbate peroxidase from spinach. *Plant Cell Physiol.* **39**, 23–34.
- Jespersen, H.M., Kjærsgård, I.V.H., Østergaard, L. and Welinder, K.G.** (1997) From sequence analysis of three novel ascorbate peroxidases from *Arabidopsis thaliana* to structure, function and evolution of seven types of ascorbate peroxidase. *Biochem. J.* **326**, 305–310.
- Jiménez, A., Hernández, J.A., del Río, L.A. and Sevilla, F.** (1997) Evidence for the presence of the ascorbate-glutathione cycle in mitochondria and peroxisomes of pea leaves. *Plant Physiol.* **114**, 275–284.
- Jones, J.M., Morrell, J.C. and Gould, S.J.** (2001) Multiple distinct targeting signals in integral peroxisomal membrane proteins. *J. Cell Biol.* **153**, 1141–1149.
- Kammerer, S., Holzinger, A., Welsch, U. and Roscher, A.A.** (1998) Cloning and characterization of the gene encoding the human peroxisomal assembly protein Pex3p. *FEBS Lett.* **429**, 53–60.
- Karnik, S.K. and Trelease, R.N.** (2005) *Arabidopsis thaliana* peroxin 16 (AtPex16p) coexists at steady state in peroxisomes and endoplasmic reticulum. *Plant Physiol.* doi: 10.1104/105.061291.
- Karyotou, K. and Donaldson, R.P.** (2005) Ascorbate peroxidase, a scavenger of hydrogen peroxide in glyoxysomal membranes. *Arch. Biochem. Biophys.* **434**, 248–257.
- Kunze, C.M., Trelease, R.N. and Turley, R.B.** (1988) Purification and biosynthesis of cottonseed *Gossypium hirsutum* L. catalase. *Biochem. J.* **251**, 147–155.
- Lisenbee, C.S., Heinze, M. and Trelease, R.N.** (2003a) Peroxisomal ascorbate peroxidase resides within a subdomain of rough endoplasmic reticulum in wild-type *Arabidopsis* cells. *Plant Physiol.* **132**, 870–882.
- Lisenbee, C.S., Karnik, S.K. and Trelease, R.N.** (2003b) Overexpression and mislocalization of a tail-anchored GFP redefines the identity of peroxisomal ER. *Traffic*, **4**, 491–501.
- López-Huertas, E., Corpas, F.J., Sandalio, L.M. and del Río, L.A.** (1999) Characterization of membrane polypeptides from pea leaf peroxisomes involved in superoxide radical generation. *Biochem. J.* **337**, 531–536.
- Luster, D.G., Bowditch, M.I., Eldridge, K.M. and Donaldson, R.P.** (1988) Characterization of membrane-bound electron transport enzymes from castor bean glyoxysomes and endoplasmic reticulum. *Arch. Biochem. Biophys.* **265**, 50–61.
- Mittova, V., Volokita, M., Guy, M. and Tal, M.** (2000) Activities of SOD and the ascorbate-glutathione cycle enzymes in subcellular compartments in leaves and roots of the cultivated tomato and its wild salt-tolerant relative *Lycopersicon pennellii*. *Physiol. Plant.* **110**, 42–51.
- Möller, S., Croning, M.D.R. and Apweiler, R.** (2001) Evaluation of methods for the prediction of membrane spanning regions. *Bioinformatics*, **17**, 646–653.
- Mullen, R.T.** (2002) Targeting and import of matrix proteins into peroxisomes. In *Plant Peroxisomes* (Baker, A. and Graham, I., eds.). Dordrecht: Kluwer Academic Publishers, pp. 339–383.
- Mullen, R.T. and Trelease, R.N.** (1996) Biogenesis and membrane properties of peroxisomes: does the boundary membrane serve and protect? *Trends Plant Sci.* **1**, 389–394.
- Mullen, R.T. and Trelease, R.N.** (2000) The sorting signals for peroxisomal membrane-bound ascorbate peroxidase are within its C-terminal tail. *J. Biol. Chem.* **275**, 16337–16344.
- Mullen, R.T., Lee, M.S., Flynn, C.R. and Trelease, R.N.** (1997a) Diverse amino acid residues function within the type 1 peroxisomal targeting signal. *Plant Physiol.* **115**, 881–889.
- Mullen, R.T., Lee, M.S. and Trelease, R.N.** (1997b) Identification of the peroxisomal targeting signal for cottonseed catalase. *Plant J.* **12**, 313–322.
- Mullen, R.T., Lisenbee, C.S., Miernyk, J.A. and Trelease, R.N.** (1999) Peroxisomal membrane ascorbate peroxidase is sorted to a membranous network that resembles a subdomain of the endoplasmic reticulum. *Plant Cell*, **11**, 2167–2185.
- Mullen, R.T., Lisenbee, C.S., Flynn, C.R. and Trelease, R.N.** (2001) Stable and transient expression of chimeric peroxisomal membrane proteins induces an independent ‘zippering’ of peroxisomes and an endoplasmic reticulum subdomain. *Planta*, **213**, 849–863.
- Murphy, M.A., Phillipson, B.A., Baker, A. and Mullen, R.T.** (2003) Characterization of the targeting signal of the *Arabidopsis* 22-kD integral peroxisomal membrane protein. *Plant Physiol.* **133**, 813–828.
- Murthy, S.S. and Zilinskas, B.A.** (1994) Molecular cloning and characterization of a cDNA encoding pea monodehydroascorbate reductase. *J. Biol. Chem.* **269**, 31129–31133.
- Ni, W., Trelease, R.N. and Eising, R.** (1990) Two temporally synthesized charge subunits interact to form the five isoforms of cottonseed (*Gossypium hirsutum*) catalase. *Biochem. J.* **269**, 233–238.
- Obara, K., Sumi, K. and Fukuda, H.** (2002) The use of multiple transcription starts causes the dual targeting of *Arabidopsis* putative monodehydroascorbate reductase to both mitochondria and chloroplasts. *Plant Cell Physiol.* **43**, 697–705.
- Olsen, L.J. and Harada, J.J.** (1995) Peroxisomes and their assembly in higher plants. *Annu. Rev. Plant Physiol.* **46**, 123–146.
- del Río, L.A., Sandalio, L.M., Corpas, F.J., López-Huertas, E., Palma, J.M. and Pastori, G.M.** (1998) Activated oxygen-mediated metabolic functions of leaf peroxisomes. *Physiol. Plant.* **104**, 673–680.
- del Río, L.A., Corpas, F.J., Sandalio, L.M., Palma, J.M., Gómez, M. and Barroso, J.B.** (2002) Reactive oxygen species, antioxidant systems and nitric oxide in peroxisomes. *J. Exp. Bot.* **53**, 1255–1272.
- Sano, S. and Asada, K.** (1994) cDNA cloning of monodehydroascorbate radical reductase from cucumber: a high degree of homology in terms of amino acid sequence between this enzyme and bacterial flavoenzymes. *Plant Cell Physiol.* **35**, 425–437.
- Sano, S., Miyake, C., Mikami, B. and Asada, K.** (1995) Molecular characterization of monodehydroascorbate radical reductase from cucumber highly expressed in *Escherichia coli*. *J. Biol. Chem.* **270**, 21354–21361.
- Soukupova, M., Sprenger, C., Gorgas, K., Kunau, W.-H. and Dodt, G.** (1999) Identification and characterization of the human peroxin PEX3. *Eur. J. Cell Biol.* **78**, 357–374.
- Tolbert, N.E., Oeser, A., Kisaki, T., Hageman, R.H. and Yamazaki, R.K.** (1968) Peroxisomes from spinach leaves containing enzymes related to glycolate metabolism. *J. Biol. Chem.* **243**, 5179–5184.
- Wang, X., Unruh, M.J. and Goodman, J.M.** (2001) Discrete targeting signals direct Pmp47 to oleate-induced peroxisomes in *Saccharomyces cerevisiae*. *J. Biol. Chem.* **276**, 10897–10905.
- Wattenberg, B. and Lithgow, T.** (2001) Targeting of C-terminal (tail)-anchored proteins: understanding how cytoplasmic activities are anchored to intracellular membranes. *Traffic*, **2**, 66–71.
- Yoon, H.-S., Lee, H., Lee, I.-A., Kim, K.-Y. and Jo, J.** (2004) Molecular cloning of the monodehydroascorbate reductase gene from *Brassica campestris* and analysis of its mRNA level in response to oxidative stress. *Biochim. Biophys. Acta*, **1658**, 181–186.
- Zacharias, D.A., Violin, J.D., Newton, A.C. and Tsien, R.Y.** (2002) Partitioning of lipid-modified monomeric GFPs into membrane microdomains of live cells. *Science*, **296**, 913–916.